Supporting information

System efficiency and power assessment of the all-aqueous copper TRAB

Nicholas R. Cross[a], Matthew J. Rau[b], Serguei N. Lvov[c,d,e], Christopher A. Gorski[f], Bruce E. Logan[a,f] , Derek M. Hall[c,d 1]

[a]Department of Chemical Engineering, Pennsylvania State University, University Park, PA 16802, USA

[b]Department of Mechanical and Aerospace Engineering, The George Washington University, Washington DC 20052, USA

[c]The EMS Energy Institute, Pennsylvania State University, University Park, PA 16802, USA

[d]Department of Energy and Mineral Engineering, Pennsylvania State University, University Park, PA 16802, USA

[e]Department of Materials Science and Engineering, Pennsylvania State University, University Park, PA 16802, USA

[f]Department of Civil and Environmental Engineering, Pennsylvania State University, University Park, PA 16802, USA

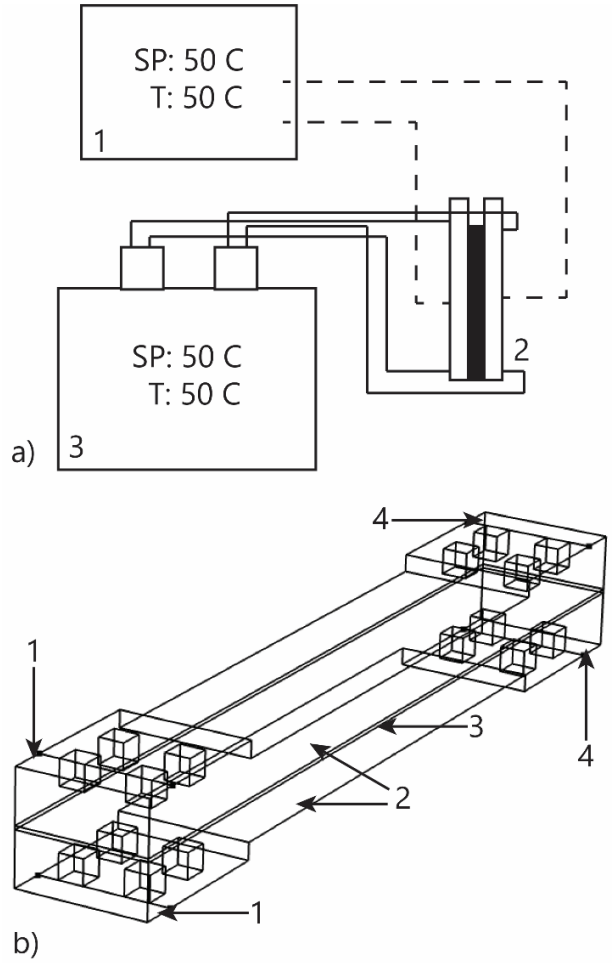

Fig. S1. a) Schematic of the elevated temperature system used for full cell tests including 1) temperature controller for the reactor stack, 2) reactor stack, and 3) oil bath for electrolyte tanks. Solid lines are for carrying electrolyte, dashed lines are for carrying electricity. b) The complete simulation domain for full cell simulations with 1) inlet boundaries, 2) symmetry boundaries, 3) membrane domain, and 4) outlet boundaries.

[1] Corresponding author: dmh5373@psu.edu

The laminar, incompressible Brinkman and continuity equations governed the fluid flow through the porous electrode are as follows

$$\frac{\rho}{\epsilon}\left(\frac{\partial \vec{u}}{\partial t} + (\vec{u}\cdot\nabla)\frac{\vec{u}}{\epsilon}\right) = -\vec{\nabla}p + \nabla\cdot\left[\frac{1}{\epsilon}\left\{\mu\left(\nabla\vec{u} + (\nabla\vec{u}^T)\right) - \frac{2}{3}\mu(\nabla\cdot\vec{u})\mathrm{I}\right\}\right], \quad (1)$$

$$\rho\nabla\cdot\vec{u} = Q_m, \quad (2)$$

where ρ is the fluid density, ϵ is the electrode porosity, $\vec{u}$ is the velocity vector, t is time, p is the fluid pressure, and Q_m is a source or sink term [1].

Both electrode domains are governed by the electroneutrality condition,

$$\sum z_i c_i = 0, \quad (3)$$

where z_i is charge of the i-th ion, and c_i is the bulk molar concentration of the i-th species. The flux and concentration change of all species in the positive channel were governed by the conservation of mass (4) and convection-diffusion (5) equations [2]:

$$\frac{\partial c_i}{\partial t} + \vec{\nabla}\cdot\vec{N}_i = 0, \quad (4)$$

$$\vec{N}_i = -D_i\vec{\nabla}c_i - \frac{z_i F}{RT}D_i c_i\vec{\nabla}\phi_e + \vec{u}c_i, \quad (5)$$

where $\vec{N}_i$ is the flux and D_i is the diffusion coefficient of an individual species, F is Faraday's constant, R is the molar gas constant, T was the temperature of the fluid, and ϕ_e was the potential of the electrolyte.

We modeled the kinetics within the porous electrode using the linearized form of the Butler-Volmer equation:

$$i_{loc} = i_0\left(\frac{(\alpha_a + \alpha_c)F}{RT}\right)\eta \quad (6)$$

where i_{loc} is the local current density, i_0 is the exchange current density of the reaction, α_a and α_c are the anodic and cathodic transfer coefficients, and η is the overpotential.

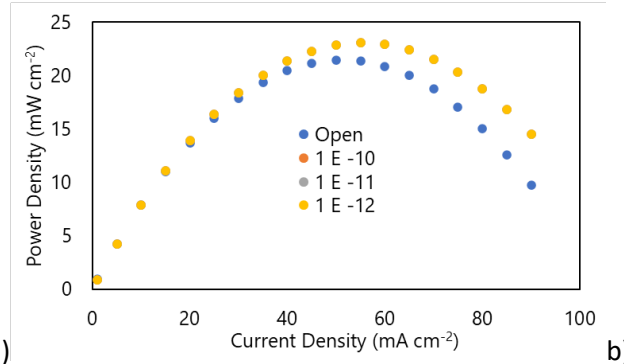

a)

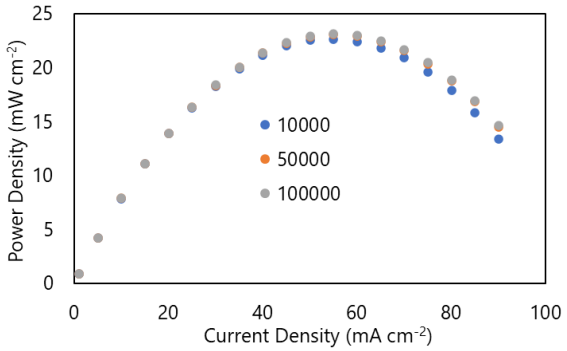

b)

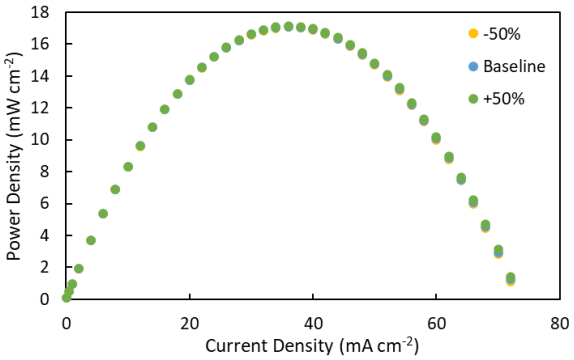

c)

Fig. S2. Sensitivity of power curves to a) electrode permeability (Open signifies the fluid flow is modeled as an open channel instead of flow through porous media), b) electrochemically active surface area, and c) copper species diffusion coefficients.

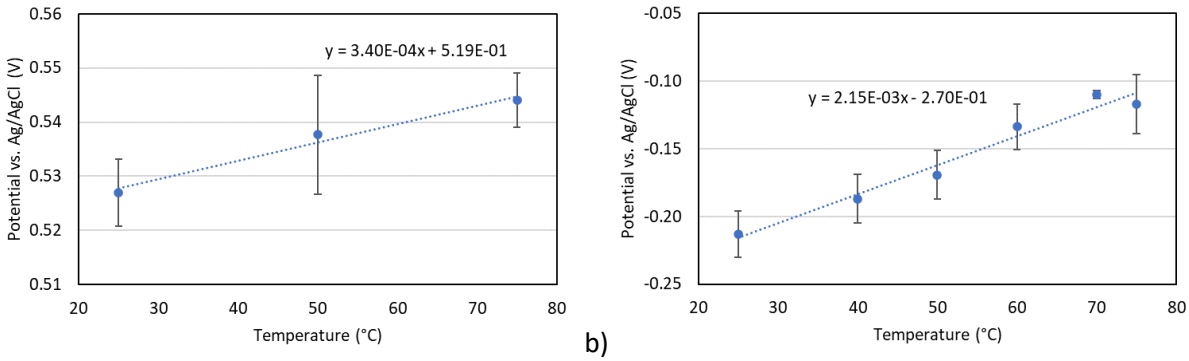

a) b)

Fig. S3. Equilibrium potential of a) positive and b) negative electrode reactions as a function of temperature

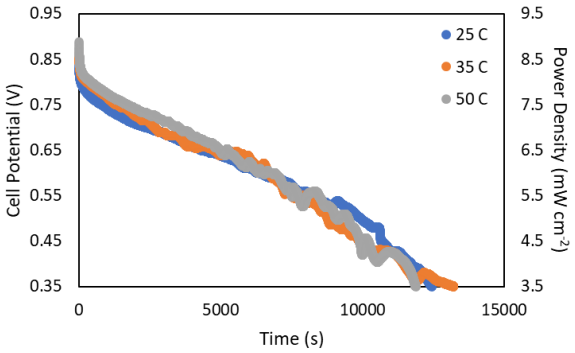

Fig. S4. Discharge curves at a range of battery operating temperatures

Table S1: Energy and efficiency results for sub-atmospheric and atmospheric columns at varying ammonia concentrations. Column energy values are at temperature where minimum total energy occurred.

Sub-Atmospheric	$\hat{u}$ (Wh L^{-1})	E_{tot} (Wh L^{-1})	E_{heat} (Wh L^{-1})	η_{tot} (%)	η_{heat} (%)	$\eta_{tot/carnot}$ (%)	$\eta_{heat/carnot}$ (%)
1 M NH_3	2.4	118	63.9	2.0	3.7	14.6	27.0
3 M NH_3	7.9	152	77.8	5.2	10.1	37.8	74.0

5 M NH_3	9.5	173	77.9	5.5	12.2	40.1	88.7
Atmospheric							
1 M NH_3	2.4	157	83.4	1.5	2.8	7.3	13.4
3 M NH_3	7.9	180	104	4.4	7.6	21.3	36.7
5 M NH_3	9.5	189	110.	5.0	8.6	24.3	41.7

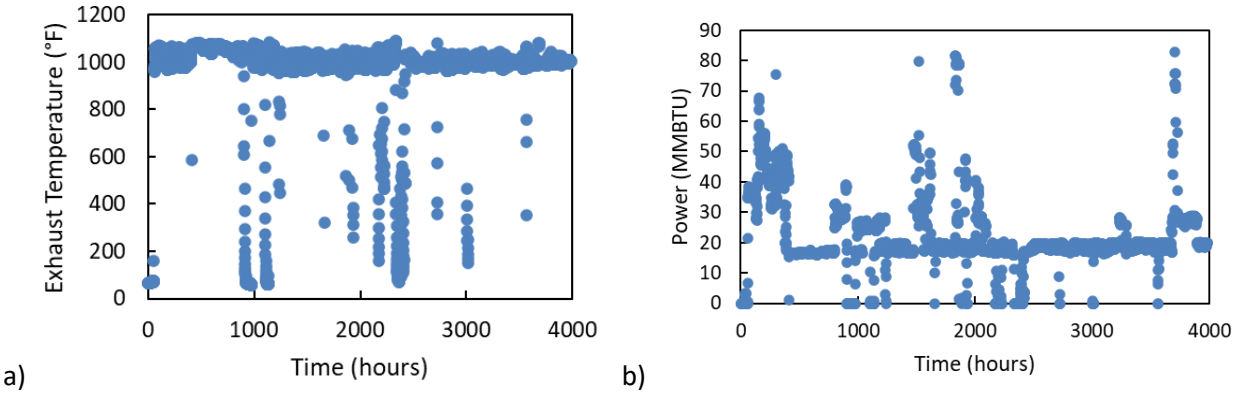

Fig. S5. Data readout of a) exhaust temperature and b) power output for Solar Turbines Taurus 60 over a year of operation

References

[1] D. Nield, A. Bejan, Convection in Porous Media, 3rd ed., Springer, 2006.

[2] J. Newman, N. Balsara, Electrochemical Systems, 4th ed., Wiley, Englewood Cliffs, 2021.